Indian Journal of Biochemistry & Biophysics
Vol. 61, May 2024, pp. 290-304
DOI: 10.56042/ijbb.v61i5.968

Lycopene enriched tomato extract exerts modulatory effects on hypoxia, angiogenesis and metastasis during N-nitrosodiethylamine (NDEA) induced hepatocellular carcinoma in mice

Chugh NA, Bhatia N, Gupta P & Koul A*

Department of Biophysics, Basic Medical Sciences Block, Panjab University, Chandigarh-160 014, Punjab, India

Received 29 April 2023; *revised 20 February 2024*

The onset and progression of hepatocellular carcinoma (HCC) is associated with several molecular and physiological changes in the tumor microenvironment. This provides a rationale for studying these changes throughout hepatic carcinogenesis and their possible modulation by putative anti-cancer agents. The present study was designed to look into the effects of lycopene enriched tomato extract (LycT) on markers linked with hypoxia, angiogenesis and metastasis at advanced stages of N-nitrosodiethylamine (NDEA) induced HCC in mice. Female balb/c mice were divided into four groups: Control, NDEA, LycT and LycT+NDEA. LycT was able to inhibit tumor formation and retard the development of histoarchitectural alterations which was consonance with the serum levels of alpha-feto protein. HCC development was associated with aggravated expression of markers linked to hypoxia (HIF), angiogenesis (VEGF, CD 31) and metastasis (MMP-2, MMP-9). LycT mediated inhibition in tumorigenesis was accompanied by decrease in expression of these markers. ^{99m}Tc-mebrofenin assay revealed diminished hepatic function in NDEA group which improved with LycT administration. These observations at late stages of HCC and those of the early stages reported previously, convincingly demonstrate that LycT effectively mitigated hepatic cancer possibly by modulating hypoxia, angiogenesis and metastasis.

Keywords: Chemoprevention, Hepatocellular carcinoma, Lycopene, *Lycopersicon esculentum*

Tumor growth and progression would not be successful without the crosstalk, connection, support and interaction with its microenvironment. Therefore, it is extremely important to study the tumor microenvironment (TME) extensively at all stages encompassing several different processes and players that may be at play. The oxygen demand in aggressively proliferating tumor tissue surpasses the oxygen supply resulting in non-physiological level of oxygen tension[1]. Increasing distance between existing vasculature and proliferating cells hampers oxygen diffusion resulting in severe hypoxic milieu. Cell division is affected by oxygen availability and more specifically G1 arrest is influenced by hypoxia-inducible factors[2,3]. Prolonged hypoxia in TME is responsible for hypervascularity that further stimulate progression and development of carcinogenesis.

Hepatocellular carcinoma (HCC) has always been a cause of worry because of its persistent position in the list of top six most deadly malignancies across the globe[4]. The onset and progression of HCC is associated with molecular and physiological transformations in the tumor and its associated microenvironment. In HCC, hypoxia plays a driving role in tumor progression and metastasis by stimulating immune invasion, angiogenesis, invasiveness *etc*. Hypoxic cancer cells acquire plasticity and non-adhesive phenotype that confers chemo- and radio-resistant properties to cancerous cells[1].

Hypoxia and the cross-talk with hypoxia associated factors plays a key role in stimulating angiogenesis followed by enhanced invasiveness that support survival of solid tumor like HCC. Hypoxia-associated rapid portal venous invasion during hepatic carcinogenesis creates immense challenges in its prognosis[5]. Obstructing the connection or hindering the interaction between TME and proliferating tumor cells makes a strong basis for developing anti-cancer approaches based on this[6]. Although, currently there are many exceedingly advanced and conventional therapies for HCC, however the global burden and morbidity of HCC is immensely worrisome[7]. Preventive strategies are as important as enhancing screening, enabling early detection, and providing

*Correspondence:
E-mail: drashwanikoul@yahoo.co.in; ashwanik@pu.ac.in

easy access to therapy for improving global outcome of HCC[8].

Epidemiological studies have revealed an inverse association between cancer risk and carotenoids. We have previously reported that lycopene enriched tomato extract (LycT) exhibited noteworthy chemopreventive potential against N-nitrosodiethylamine (NDEA) induced HCC in mice. This was associated with modulation of cell proliferation, cell death, glycolytic enzymes, hepatic ultrastructure, and chromosomal aberrations *etc*[9-12]. We also reported that LycT exhibited attenuating effects on expression of important molecules linked to hypoxia, angiogenesis and metastasis during initial stages of NDEA induced HCC in mice[13]. The results related to TME observed at initial stages of HCC encouraged us to evaluate possible molecular changes at advanced/later stages as well. Thus, the present study was designed to look into the effects of LycT on hypoxia, angiogenesis and metastasis at advanced stages of HCC in mice.

Materials and Method

Chemicals

2,2'-azino-bis(3-ethylbenzthiazoline-6-sulphonic acid) (ABTS), diethylpyrocarbonate (DEPC), ethidium bromide (EtBr), N-nitrosodiethylamine (NDEA), tri-reagent were obtained from Sigma Aldrich (USA). Primary antibodies against HIF-1α, VEGF, CD31, MMP-9 and MMP-2 and horse radish peroxidase conjugated anti-rabbit secondary antibody were purchased from Santa Cruz Biotechnology (USA). One-step reverse transcription polymerase chain reaction (RT-PCR) kit was obtained from Invitrogen (USA). Primers (oligonucleotides; Table 1) used in RT-PCR were procured from Sigma Aldrich (USA). Molecular biology grade chemicals for RNA isolation were purchased from Amresco (USA). Other chemicals utilized in the present study were procured from reputed Indian manufacturers and were of the highest purity grade. ELISA kit for determining alpha fetoprotein (AFP) levels was procured from WKEA Med Supplies (China). Red tomatoes (*Lycopersicon esculentum*) were procured from local market and kept refrigerated until use. Mebrofenin kit was procured from Board of Radiation Isotope Technology (BRIT), Mumbai (India).

Preparation of lycopene enriched tomato extract (LycT)

LycT was prepared in our laboratory using red tomatoes by following the previously described method that used hexane/acetone/ethanol (2:1:1) as the extraction medium[9]. The extract was reconstituted in olive oil prior to its administration to the animals. Both carotenoids and non-carotenoids have been observed to be present in tomato extracts. Lycopene is the predominant constituent among the carotenoids while waxes, fatty acids, phospholipids and acylglycerols are some of the non-carotenoids. This extract has been previously characterized using NMR and FT-IR which revealed the presence of structural groups of lycopene. As evident from UV-visible spectroscopy, the extract exhibited absorption maxima at 444, 470 and 503 nm. To avoid interference from other carotenoids, the content of lycopene in this extract was quantified using the optical density values at 503nm with an extinction coefficient of 1.72×10^5 M^{-1} cm^{-1}. The average lycopene content was found to be around 11-14 mg/kg of tomatoes[9]. We have previously demonstrated that this extract exhibited dose dependent radical scavenging effects in *in vitro* assays such as 1, 1-Diphenyl-2-picrylhydrazyl (DPPH)

Table 1 — List of primer pairs used for RT-PCR

Gene	Strand	Primer	Reference/Accession No.
HIF-1α	Sense	5′-GGTCAGATGATCAGAGTCCA-3′	
	Antisense	5′-TGCTTGGTGCTGATTTGTGA-3′	[47]
VEGF	Sense	5'-TCTTCAAGCCATCCTGTGTG-3'	
	Antisense	5′-ATCCGCATAATCTGCATGGT-3′	[48]
CD31	Sense Antisense	5'-GACACTACACCTGCAAAGTG-3'	
		5′-GCACCGAAGTACCATTTCAC-3′	[49]
MMP-2	Sense	5′-ACCCTAGGGGATGCTTGGAT-3′	
	Antisense	5′-ACGAGCGAAGGGCATACAAA-3′	NM_008610.2
MMP-9	Sense	5′-TTCACCGGCTAAACCACCTC-3′	
	Antisense	5′-TAACGCCCAGTAGAGAGCC-3′	NM_013599.2
β-actin	Sense Antisense	5′-ATCCGTAAAGACCTCTATGC-3′	
		5′-AACGCAGCTCAGTAACAGTC-3′	[50]

assay, ABTS assay and DNA damage inhibition assay[14].

Procurement of animals and experimental conditions

Female Balb/c mice in the weight range of 25-30g were procured from Central Animal House, Panjab University, Chandigarh and housed in a well ventilated room maintained at a temperature of 21 ± 1ºC. All the mice were provided standard animal pellet diet (Ashirwad Industries Ltd., Ropar, Punjab, India) and drinking water *ad libitum* till the end of treatment period. The experimental studies were approved by Institutional Animal Ethics Committee (IAEC), Panjab University, Chandigarh (India) and executed in compliance with the Indian National Science Academy Guidelines for the use and care of experimental animals (IAEC/284-295 at Sr. No. 47). The mice were acclimatized to the experimental conditions for one week prior to the commencement of various treatments. The final day of this period was considered as week zero of the experiment.

NDEA induced hepatocarcinogenesis and its chemoprevention by LycT

After acclimatization, the mice were randomly divided into four groups (n=10-15) based upon the treatment they were assigned. Animals in control group (group 1) were orally administered with olive oil (vehicle for LycT) three times a week for 24 weeks. Animals in NDEA group (group 2) received a weekly intraperitoneal dose of NDEA for 8 weeks (cumulative dose of 200mg/kg body weight, dissolved in 0.9% normal saline). Animals of LycT group (group 3) were orally administered with LycT dissolved in olive oil at a dose of 5 mg/kg body weight three times a week till the termination of the experimental period (*i.e*. 24 weeks). Mice of LycT + NDEA group (group 4) were administered with LycT and NDEA as explained for groups 2 and 3. In LycT + NDEA group, NDEA treatment was commenced after two weeks of LycT treatment. The dose regimen of NDEA for hepatocarcinogenesis and its chemoprevention by LycT adopted in the present study was based on our previous reports[9-13,15].

Investigations in serum and hepatic tissue were done at two time points (16^{th} and 24^{th} week). 16^{th} week represented the promotion stage whereas 24^{th} week represented the progression stage of HCC development. A weekly record of body weight was maintained and hepatosomatic index was determined as the ratio of liver weight to the total body weight of animals.

Tumor assessment

After the completion of treatment, the animals were sacrificed by cervical dislocation and liver was excised. The livers were carefully observed for the presence of tumors and accordingly various tumor related parameters were evaluated[9].

Histopathological studies

At 16 and 24 weeks, the excised hepatic tissues were immediately fixed in buffered formalin and then processed using the procedure described previously[16]. Following fixation, the tissues were made to undergo dehydration by subjecting them to ascending concentration of alcohol, followed by clearing with benzene and then infiltration and embedding with paraffin wax. After this, serial sections (five micrometer thickness) were cut using a rotary microtome, placed on glass slides and these were then used for hematoxylin and eosin (H&E) staining. Stained sections were mounted and viewed under light microscope (LEICA DM 3000).

Assessment of serum alpha-feto protein (AFP)

At 16 and 24 weeks, serum was prepared from the blood withdrawn from the ocular vein (retro-orbital plexus) of mouse eye. Quantitative estimation of AFP in serum was carried out using solid phase enzyme linked immunosorbent assay following the instructions mentioned in the kit protocol.

Assessment of mRNA expression using Reverse transcriptase polymerase chain reaction analysis (RT-PCR)

The mRNA expression analysis of various genes linked to hypoxia (hypoxia inducible factor, HIF-α), angiogenesis [vascular endothelial growth factor (VEGF)], [cluster of differentiation-31 (CD-31)] and metastasis [matrix metalloproteinases (MMP-9, MMP-2)] was carried out at 16 and 24 weeks using end-point RT-PCR. Total RNA was isolated from hepatic tissues using tri-reagent. It's purity, integrity and concentration was checked by taking absorbance at 260 and 280 nm and finding their ratio. The RT-PCR reaction mixture was prepared adhering to the kit manufacturer's instructions. The reaction was carried out in a thermal cycler with the following conditions of temperature and time being followed at the various steps: reverse transcription (50°C, 50 min), activation (95°C, 1 min), followed by 35 cycles of denaturation (94°C, 45 sec), annealing

(variable temperature, 45 sec), extension (72°C, 1 min) and lastly final extension (72°C, 10 min). To analyze the final PCR products, horizontal agarose gel electrophoresis was carried out and the bands obtained were evaluated for their densitometric values by Image J software (NIH, USA). β-actin was used as a loading control.

Assessment of protein expression using ELISA

At 16 and 24 weeks, nuclear and cytoplasmic extracts were prepared from the liver tissue according to the previously described method[17,18]. Protein quantification in these extracts was done using the method described earlier[19]. The nuclear extract was used for the protein expression analysis of HIF-1α while cytoplasmic extract was used for VEGF and CD31. MMP-9 & MMP-2 were analyzed in the homogenate of the hepatic tissues. The antigen present in the sample was immobilized onto the ELISA strip wells, which was followed by incubation with the primary antibody of interest. This was followed by incubation with horseradish-peroxidase (HRP) labelled secondary antibody. Washing steps were carried out appropriately with a buffered detergent solution and buffer to remove any proteins or antibodies that may have bound non-specifically. Incubation in dark was carried out with a substrate specific for HRP (2,2'-azino-bis(3-ethylbenzthiazoline-6-sulphonic acid) [ABTS] and H_2O_2) and the coloured reaction product formed was quantified using a microstrip reader at 405nm (STAT FAX 325+, Awareness Technology Inc., USA).

Enzymatic analysis of matrix metalloproteinases (MMPs) by gelatin zymography

At 16 and 24 weeks, the gelatinolytic activity of MMP-2 and MMP-9 in serum was performed according to the method described previously with minor modifications[20]. Serum samples were separated on gelatin-impregnated, polyacrylamide gel under non-reducing conditions, followed by shaking in renaturing buffer. The gels were then incubated in developing buffer and stained with amido black. The bands obtained after zymography were analysed quantitatively by Image J software (NIH, USA).

Assessment of hepatobiliary function

Hepatobiliary function test was carried at 16 and 24 weeks to evaluate hepatic function, biliary obstruction and hepatic extraction fraction using ^{99m}Tc-mebrofenin[15]. The labeling of mebrofenin with ^{99m}Tc was done in the Department of Nuclear Medicine, PGIMER, Chandigarh. Mice were intravenously administered with ^{99m}Tc- sodium pertechnetate labelled mebrofennin and immediately placed over the scintillation counter with liver and mediastinum in the field of view. Liver activity of ^{99m}Tc- sodium pertechnetate labelled mebrofenin was determined over time and then used to calculate the percentage of activity retained by the hepatic tissue (hepatic retention). The time required for maximum uptake of mebrofenin (T_{peak}) as well as the time at which the activity reduces to its half ($T_{1/2\ peak}$) was also calculated for the hepatic tissue.

Statistical Analysis

Data was expressed as mean ± standard deviation (SD). Statistical significance for tumor bioassay parameters was analyzed using student's unpaired t-test and for the other parameters one-way analysis of variance (ANOVA) followed by Duncan's post hoc test was used ($P \leq 0.05$).

Results

Hepatosomatic Index

At 16 and 24 weeks, a marked increase in hepatosomatic index was observed in NDEA group when compared to the control and LycT groups (Fig. 1A). Hepatosomatic index was observed to be decreased in LycT+NDEA group when compared to NDEA group and remained unaltered when compared to control and LycT groups. No changes were observed between LycT and control groups (Fig. 1B).

Macroscopic Examination of Liver

Animals of control and LycT groups did not show any alteration in the gross morphology of liver. Left, right, medium and caudate lobes were distinguishably visible. NDEA treatment to mice caused alterations in the gross morphology of liver in NDEA and LycT + NDEA groups. Tumor nodules began to appear in the liver of NDEA group by the end of 10 weeks, however, in LycT + NDEA group, visible tumor nodules were observed by the end of 16 weeks. Liver of NDEA group was characterized by undistinguished liver lobes with regenerated outgrowths, roughening of liver surface and appearance of dark and light patches. The dark patches typically characterized an increased liver vascularisation following NDEA treatment. In contrast, animals of LycT + NDEA group showed the presence of four distinguishable lobes (Fig. 2).

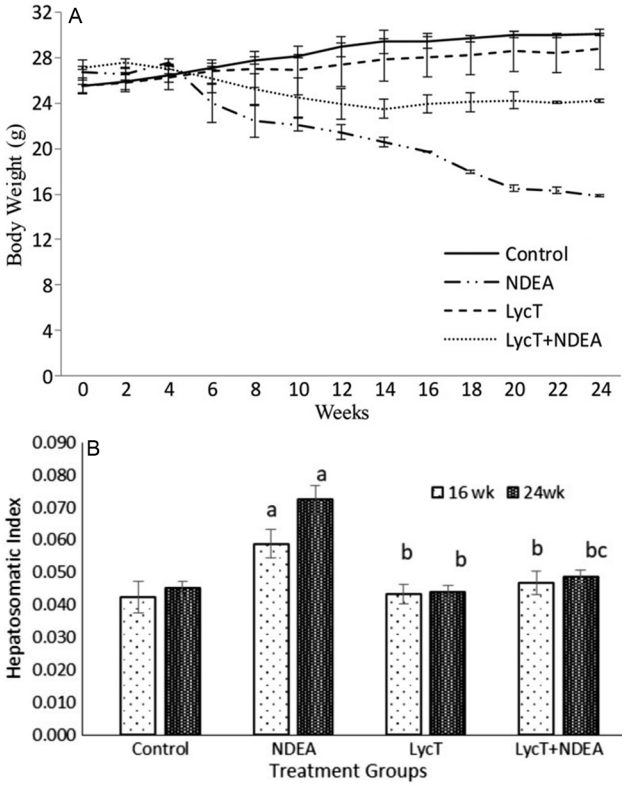

Fig. 1 — (A) Bodyweight during NDEA induced carcinogenesis and its chemoprevention by LycT Data is represented as Mean±SD and analysed by Student's paired t-test; and (B) Hepatosomatic index during NDEA induced hepatocarcinogenesis and its chemoprevention by LycT Data is represented as Mean±SD and analysed by One Way ANOVA followed by post-hoc test. [a]$P \leq 0.05$ significant wrt control group; [b]$P \leq 0.05$ significant wrt NDEA group; [c]$P \leq 0.05$ significant wrtLycT group

Tumor Statistics

Tumor incidence was observed to be 89.4% in NDEA group which was reduced to 53.3% in LycT+NDEA group. Animals of NDEA group revealed a tumor multiplicity of 4.97 ± 4.21 which was reduced to 2.04 ± 2.14 in LycT+NDEA group. Tumorburden also decreased in LycT+NDEA group when compared to NDEA group. The size and number of tumors also exhibited an appreciable decrease in LycT+NDEA group (Table 2).

Hepatic Tumor Marker (Alpha- fetoprotein-AFP)

Serum level of AFP at 16 and 24 weeks exhibited a significant increase in NDEA group when compared to control and LycT groups. AFP level decreased in Lyct+NDEA group when compared to NDEA group and increased when compared to control and LycT groups. No changes were observed between LycT and control groups (Fig. 3).

Histoarchitectural Analysis

H&E stained sections of hepatic tissue obtained from control and LycT groups exhibited normal histoarchitecture with no visible abnormalities. Hepatic lobules, central vein, portal vein, portal triad, hepatocytes, sinusoids arranged in a regular fashion were evident (Fig. 4).

NDEA administration induced a marked disruption in the hepatic histoarchitecture in animals of both NDEA and LycT + NDEA groups. At the end of 16th week, liver sections from animals of NDEA and LycT + NDEA groups revealed extensive hepatocellular

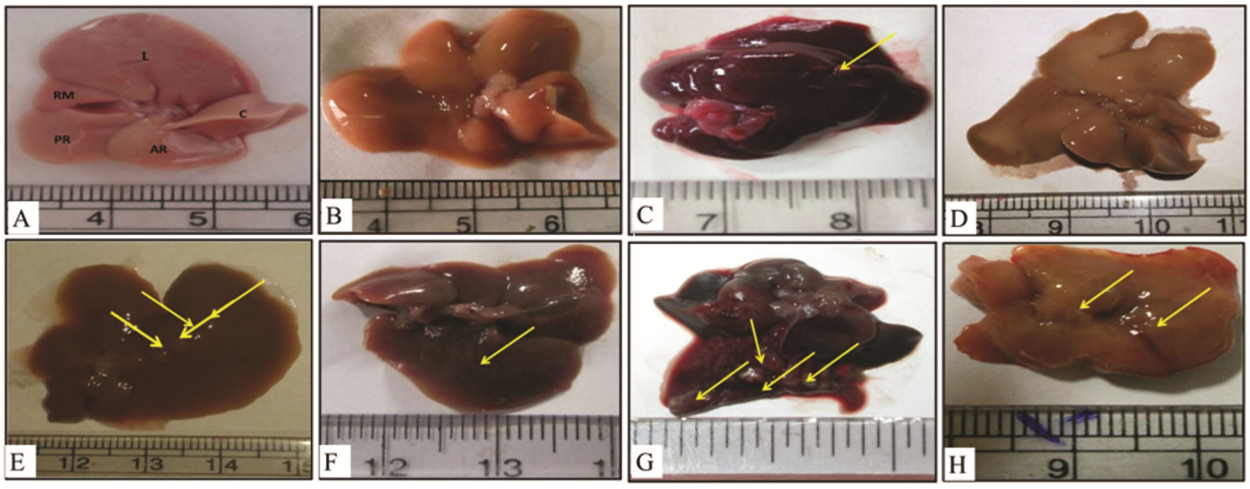

Fig. 2 — Gross morphology of liver from different groups during NDEA induced hepatocarcinogenesis. (A & B) represent liver from control and LycT groups respectively; (C & D) represent liver from NDEA and LycT + NDEA groups respectively at 10th week; (E & F) represent liver from NDEA and LycT + NDEA groups respectively at 16th week; and (G & H) represent liver from NDEA and LycT + NDEA groups respectively at 24th week. (L= left lobe; RM= right medium lobe; PR= Posterior right lobe; C= caudate lobe; AR= anterior right lobe).

Table 2 — Effect of LycT on NDEA induced hepatocarcinogenesis

Groups	Big Tumor (≥3mm)	Small Tumor (<3mm)	Tumor Incidence	Tumor Multiplicity	Tumor Burden
Control	Nil	Nil	Nil	Nil	Nil
NDEA	62	45	89.4	4.97±4.21 (0-16)	5.63
LycT	Nil	Nil	Nil	Nil	Nil
LycT+NDEA	16	35	53.3	2.04±2.14* (0-5)	3.4

Data is represented as Mean±SD (n=15) and analysed by Student's t-test. *$P \leq 0.05$ significant wrt NDEA group

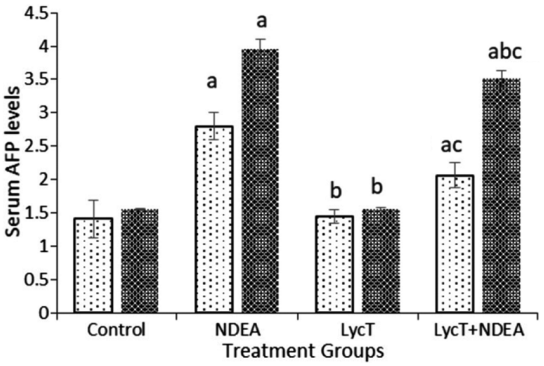

Fig. 3 — Serum AFP levels during NDEA induced hepatocarcinogenesis and its chemoprevention by LycT Data is represented as Mean±SD (n=6) and analysed by One Way ANOVA followed by post-hoc test. [a]$P \leq 0.05$ significant wrt control group; [b]$P \leq 0.05$ significant wrt NDEA group; [c]$P \leq 0.05$ significant wrt LycT group

damage. NDEA group showed the development of well to moderately differentiated HCC. Highly distorted hepatic histoarchitecture with increased regions of eosinophilic stain, focal necrosis, hyperplasia, 3-4 cell plate thickening, distorted central vein and irregular sinusoids were visible. Vascular invasion into the portal triad was also observed. Smaller size hepatocytes were visible with increased vacuolization in cytoplasm, large hyperchromatic nucleus and multiple nucleoli. LycT + NDEA group at 16th week showed the development of high grade dysplastic nodules to well differentiated HCC. The tissue sections showed architectural atypia which was characterized by the presence of smaller size hepatocytes with nuclear crowding and increased eosinophilic cytoplasm. No invasion of portal tract was observed in animals of LycT + NDEA group. NDEA group at the end of 24th week showed the conversion of well or moderately differentiated HCC to poorly or undifferentiated HCC. HCC was characterized by the formation of tumor nodules with a clear fibrous capsule. Tumor cells were rounded or spindle in shape, with scanty cytoplasm and hyperchromatic nucleus. However, the size of tumor cells was much smaller than the normal hepatocytes. An enormous increase in cell density was also evident. Cells typically formed a nest like pattern with the absence of sinusoidal spaces in between the cells. No trabecular pattern was observed. However, liver sections from animals of LycT + NDEA group at 24th week represented well differentiated HCC with stromal invasion into the portal tract. Irregular trabecular pattern was observed (Fig. 5).

Assessment of functional status of hepatic tissue

At 16th week, liver from control and LycT groups showed similar uptake, retention and excretion of ^{99m}Tc-Mebrofenin activity. This was supported by similar T_{peak} (5.0-6.0 min) and $T_{1/2peak}$ (7.0-8.0 min) values in both the groups. Liver biokinetics data demonstrated that only 3.0-6.0% of the injected dose was retained at 60 min post administration. The delay in hepatic uptake of ^{99m}Tc-mebrofenin was more pronounced in liver from NDEA group as showed by peak uptake at 22 min. However, T_{peak} was reduced to 6.0 min in LycT + NDEA group. $T_{1/2peak}$ in liver of LycT + NDEA group was observed at around 16 min, while, no $T_{1/2\ peak}$ value was obtained for liver of NDEA group. At 60 min post administration, 74.0% of the injected dose of the radiotracer was retained in liver of NDEA group which was reduced to 26.0% upon LycT supplementation to NDEA treated mice. When assessed at 24th week, at 60 min post administration of ^{99m}Tc-mebrofenin, 4.0-5.0% of the injected dose was retained in liver of control and LycT groups. In NDEA group, 82.0% of the injected dose retained in the liver at 60 min post injection which suggested a significant malfunctioning of hepatocyte. T_{peak} of ^{99m}Tc-Mebrofenin was observed at around 5.0-6.0 min in the liver of both control and LycT groups. However, in NDEA group, T_{peak} was observed in liver at around 18 min which was reduced to 7.0 min upon LycT administration to NDEA treated mice. Liver of control and LycT groups showed $T_{1/2\ peak}$ at around 7.0-8.0 min, while, $T_{1/2\ peak}$ was observed at 21 min in liver of LycT + NDEA group. However, liver of NDEA group did not show $T_{1/2\ peak}$, thus, showing the slow excretion of ^{99m}Tc-mebrofenin (Fig. 6).

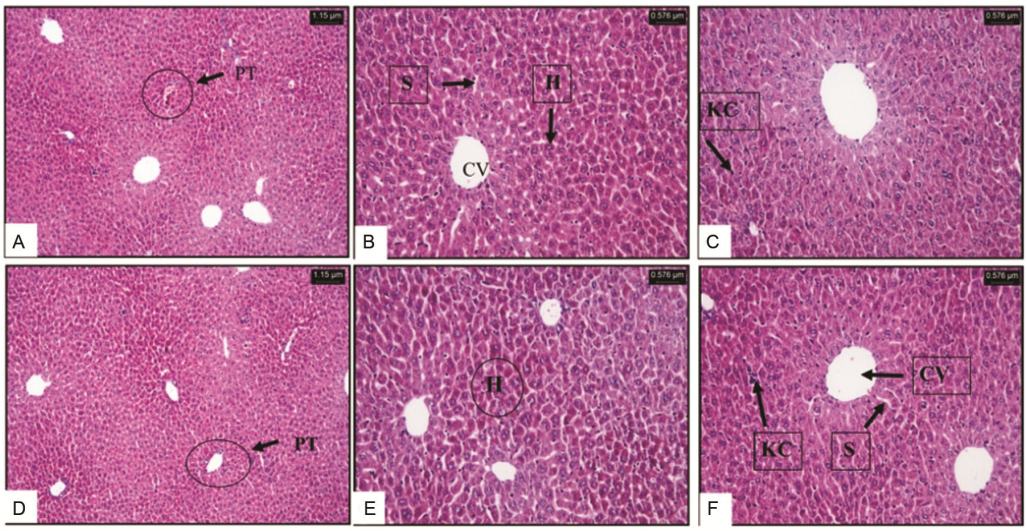

Fig. 4 — Hematoxylin and Eosin stained sections of liver from control and LycT groups illustrating normal histoarchitecture of hepatic tissue with the presence of normal central vein (CV); portal triad showing bile duct (BD), hepatic portal vein (PV) and hepatic artery (PA); hepatocytes (H); kupffer cells (KC) and sinusoids (S) Control group (A-C; 100, 200, 400x); LycT group (D-F; 100, 200, 400x)

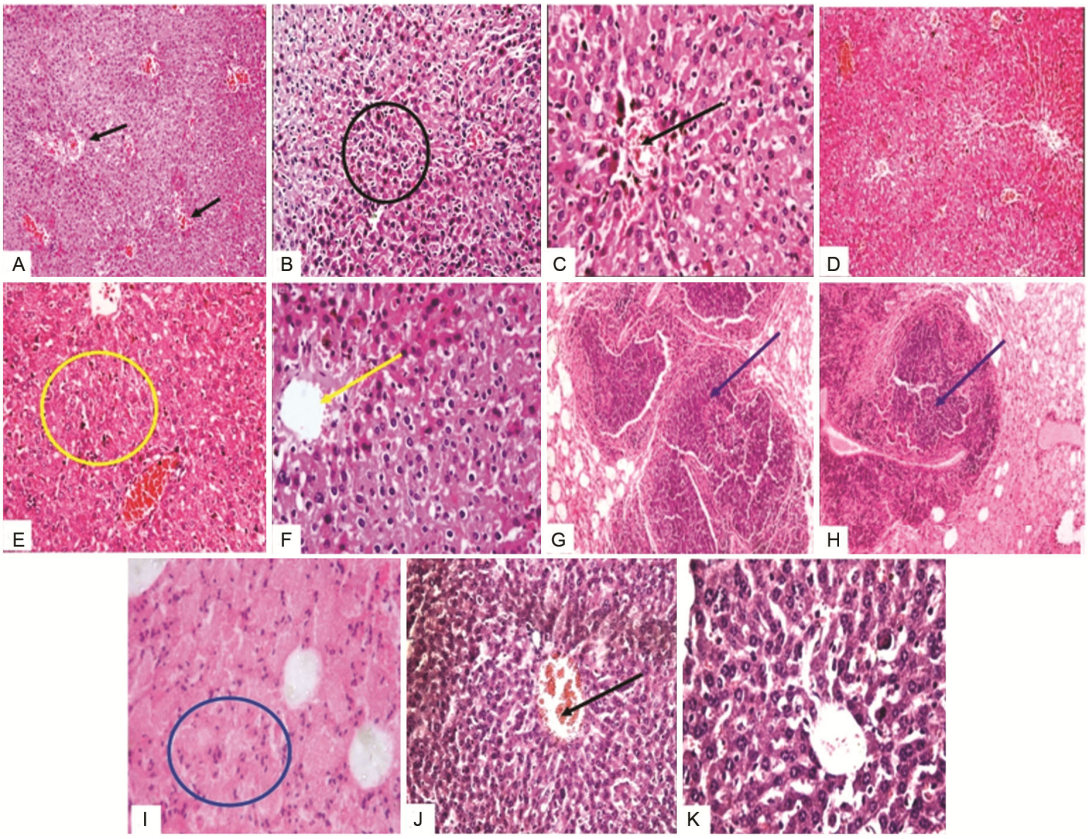

Fig. 5 — Hematoxylin and Eosin stained sections of liver from NDEA and LycT+NDEA groups (A-C; 100, 200, 400x; NDEA 16 weeks) showing extensive hepatocellular damage, well to moderately differentiated HCC (black circle), thin trabecular pattern, distorted central vein, hyperplasia, irregular sinusoids pattern, decreased cell size and stromal invasion (black arrow); (D-F; 100, 200, 400x; LycT+NDEA 16 weeks) showing high grade dysplasia to well differentiated HCC, architectural atypia (yellow circle) and no stromal invasion (yellow arrow); (G-I; 100, 200, 400x; NDEA 24 weeks) showing poorly differentiated to undifferentiated HCC with nest of hepatocytes surrounded by fibrous encapsulation (blue arrow), enormous tumor cell density and nuclear crowding (blue circle); (J-K; 200, 400x; LycT+NDEA 24 weeks) showing well differentiated HCC with stromal invasion into the portal tract (black arrow)

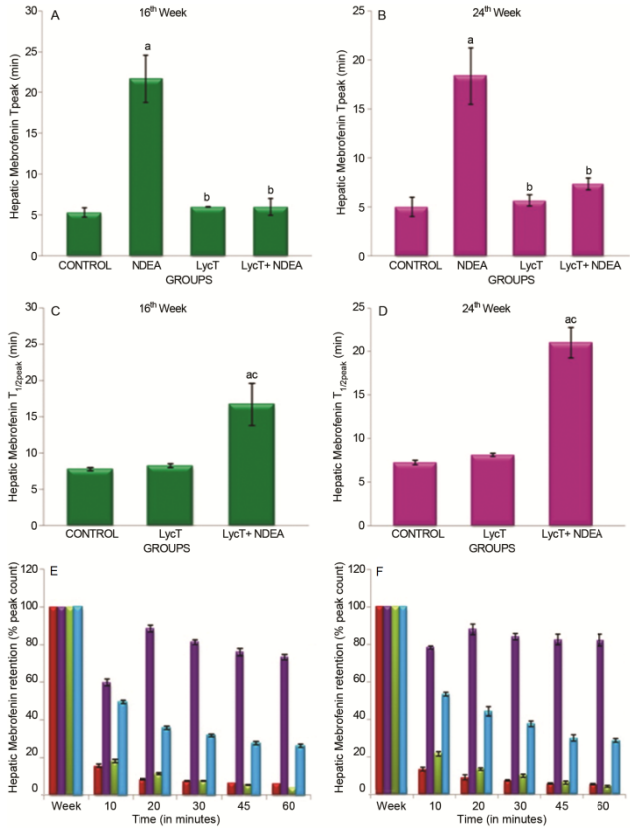

Fig. 6 — Hepatobiliary function assessed from ^{99m}Tc-mebrofenin assay T peak (A & B); T1/2 peak; (C & D); hepatic retention at 16 and 24 weeks; (E & F) Data is represented as Mean±SD (n=6) and analysed by One Way ANOVA followed by post-hoc test. $^{a}P \leq 0.05$ significant wrt control group; $^{b}P \leq 0.05$ significant wrt NDEA group; $^{c}P \leq 0.05$ significant wrt LycT group

mRNA expression of hypoxia, angiogenesis and metastasis associated genes

Vascular endothelial growth factor (VEGF) and Cluster of differentiation (CD)-31

A similar trend of alterations was observed for mRNA expressions of VEGF and CD-31. At 16 and 24 weeks, NDEA group exhibited a significant increase in mRNA expression of these genes when compared to control and LycT groups. LycT + NDEA group exhibited marked increase in expression when compared to control and LycT groups and decreased when compared to NDEA group. mRNA expression of these genes did not differ between the animals of LycT and control groups (Fig. 7A & B).

***Hypoxia Inducible Factor-α* (HIF-α)**

At 16 and 24 weeks, NDEA group exhibited a significant increase in mRNA expression of HIF-α when compared to control and LycT groups. LycT + NDEA group exhibited marked increase in expression of HIF-α when compared to control group and decreased when compared to NDEA group. mRNA expression of HIF-α did not differ between the animals of LycT and control groups (Fig. 7C).

Matrix metalloproteinase-9 (MMP-9)

At 16 and 24 weeks, NDEA group exhibited a significant increase in mRNA expression of MMP-9 when compared to control and LycT groups. LycT + NDEA group exhibited marked increase in expression of MMP-9 when compared to control group and

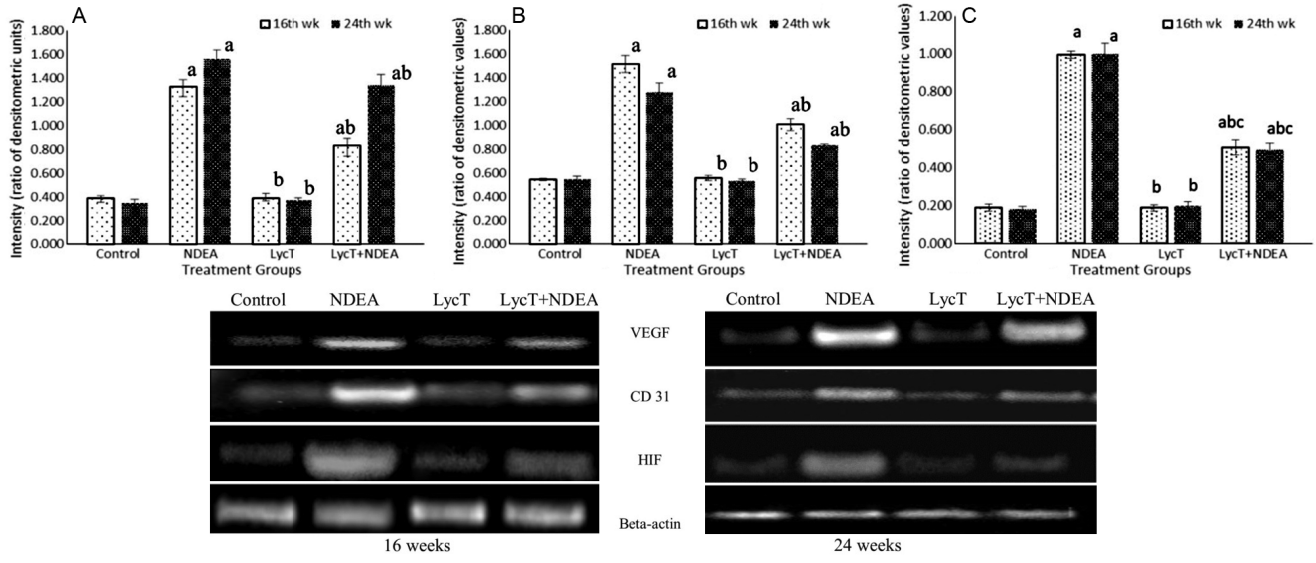

Fig. 7 — mRNA expression of genes associated with angiogenesis and hypoxia during NDEA induced hepatocarcinogenesis and its chemoprevention by LycT Densitometric analysis of bands obtained after RT-PCR (A) VEGF; (B) CD 31; and (C) HIF-α Data is represented as Mean±SD (n=6) and analysed by One Way ANOVA followed by post-hoc test. $^{a}P \leq 0.05$ significant wrt control group; $^{b}P \leq 0.05$ significant wrt NDEA group; $^{c}P \leq 0.05$ significant wrt LycT group

decreased when compared to NDEA group. mRNA expression of MMP-9 did not differ between the animals of LycT and control groups (Fig. 8A).

Matrix metalloproteinase-2 (MMP-2)

At 16 and 24 weeks, NDEA group exhibited a significant increase in mRNA expression of MMP-2 when compared to control and LycT groups. LycT + NDEA group exhibited marked increase in expression of MMP-2 when compared to control group and decreased when compared to NDEA group. mRNA expression of MMP-2 did not differ between the animals of LycT and control groups [Fig. 8B).

Enzymatic activity of matrix associated enzymes

MMP-9

At 16 and 24 weeks, NDEA group exhibited a significant increase in enzymatic activity of MMP-9 when compared to control and LycT groups. LycT + NDEA group exhibited marked increase in activity of MMP-9 when compared to control group and decreased when compared to NDEA group. Enzymatic activity of MMP-9 did not differ between the animals of LycT and control groups (Fig. 8C).

MMP-2

At 16 and 24 weeks, NDEA group exhibited a significant increase in enzymatic activity of

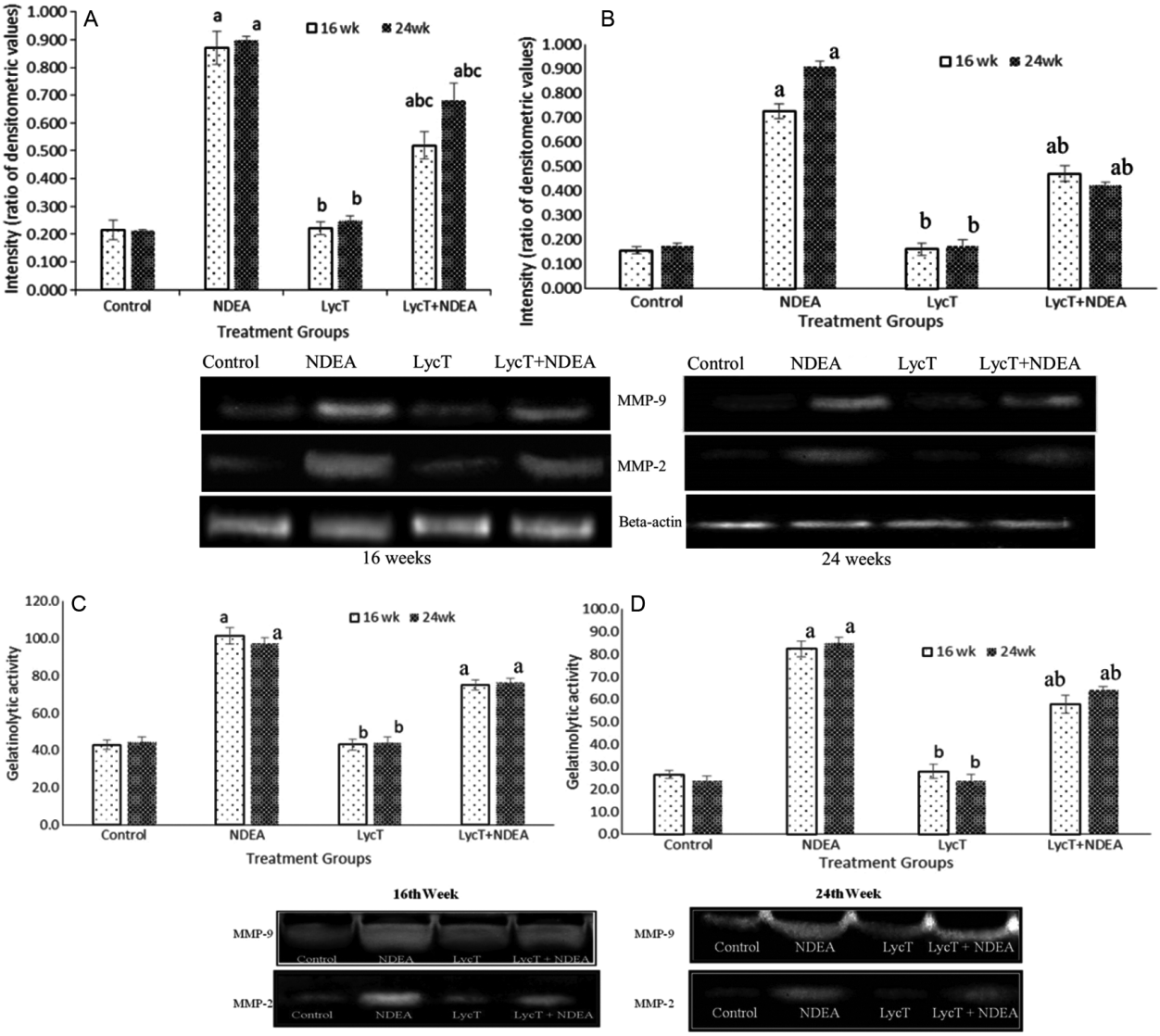

Fig. 8 — Modulation of metastasis associated genes during NDEA induced carcinogenesis and its chemoprevention by LycTDensitometric analysis of bands obtained RT-PCR of (A) MMP-9; (B) MMP-2. Gelatinolytic activity assessed by zymography; and (C) MMP-9 (D) MMP-2 Data is represented as Mean±SD (n=6) and analysed by One Way ANOVA followed by post-hoc test. [a]$P \leq 0.05$ significant wrt control group; [b]$P \leq 0.05$ significant wrt NDEA group; [c]$P \leq 0.05$ significant wrt LycT group

MMP-2 when compared to control and LycT groups. LycT + NDEA group exhibited marked increase in activity of MMP-2 when compared to control group and decreased when compared to NDEA group. Enzymatic activity of MMP-2 did not differ between the animals of LycT and control groups (Fig. 8D).

Protein expression of hypoxia, angiogenesis and metastasis associated genes

VEGF and CD-31

A similar trend of alterations was observed for protein expressions of VEGF and CD-31. At 16 and 24 weeks, NDEA group exhibited a significant increase in protein expression of these genes when compared to control and LycT groups. LycT + NDEA group exhibited marked increase in expression of VEGF and CD-31 when compared to control and LycT groups and decreased when compared to NDEA group. Protein expression of VEGF did not differ between the animals of LycT and control groups (Fig. 9A & B).

HIF-*α*

At 16 and 24 weeks, NDEA group exhibited a significant increase in mRNA expression of HIF-α

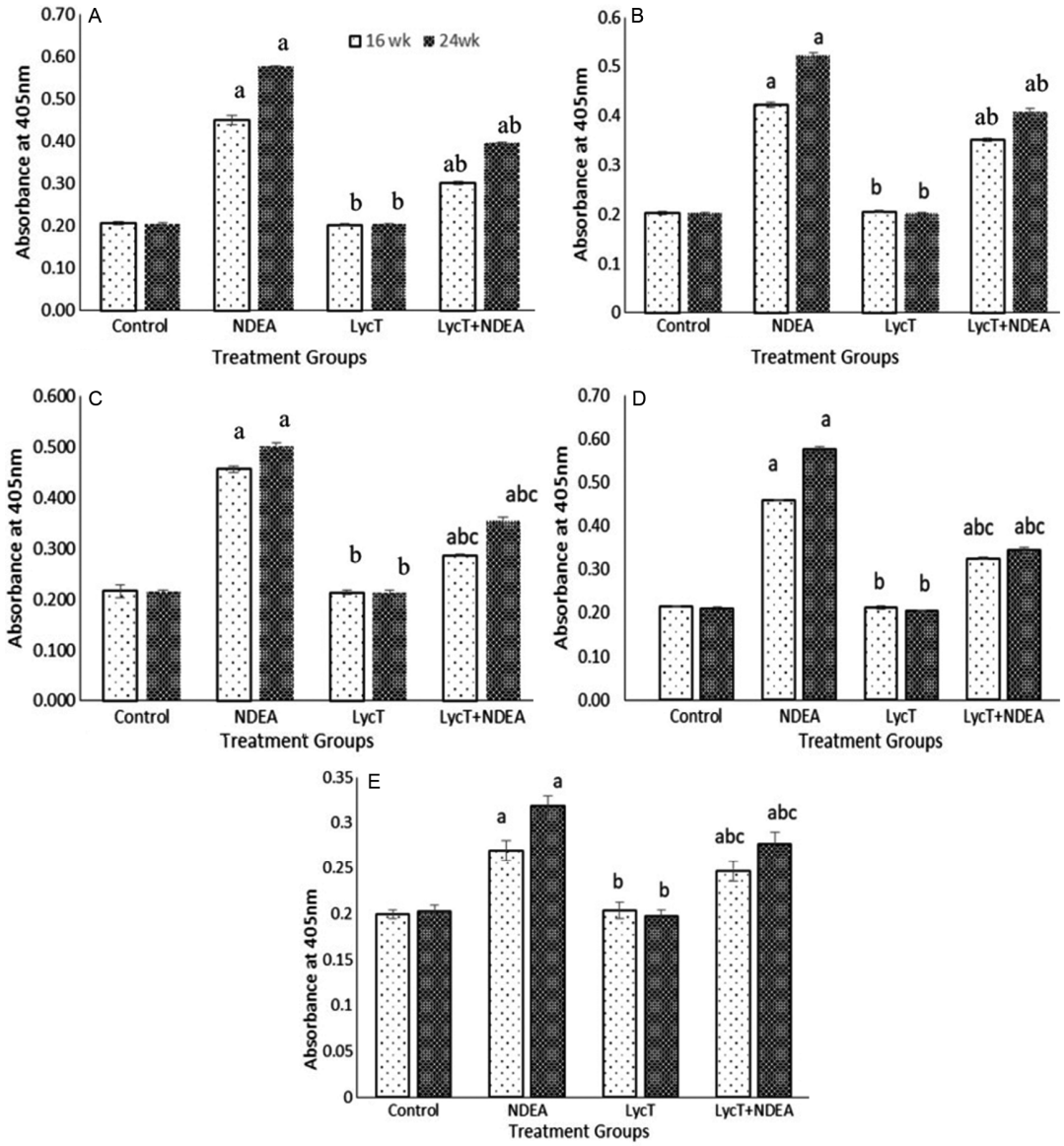

Fig. 9 — Protein expression of genes associated with angiogenesis, hypoxia and metastasis during NDEA induced hepatocarcinogenesis and its chemoprevention by LycT (A) VEGF; (B) CD- 31; (C) HIF- α; (D) MMP-9; and (E) MMP-2 Data is represented as Mean±SD (n=6) and analysed by One Way ANOVA followed by post-hoc test. [a]$P \leq 0.05$ significant wrt control group; [b]$P \leq 0.05$ significant wrt NDEA group; [c]$P \leq 0.05$ significant wrt LycT group

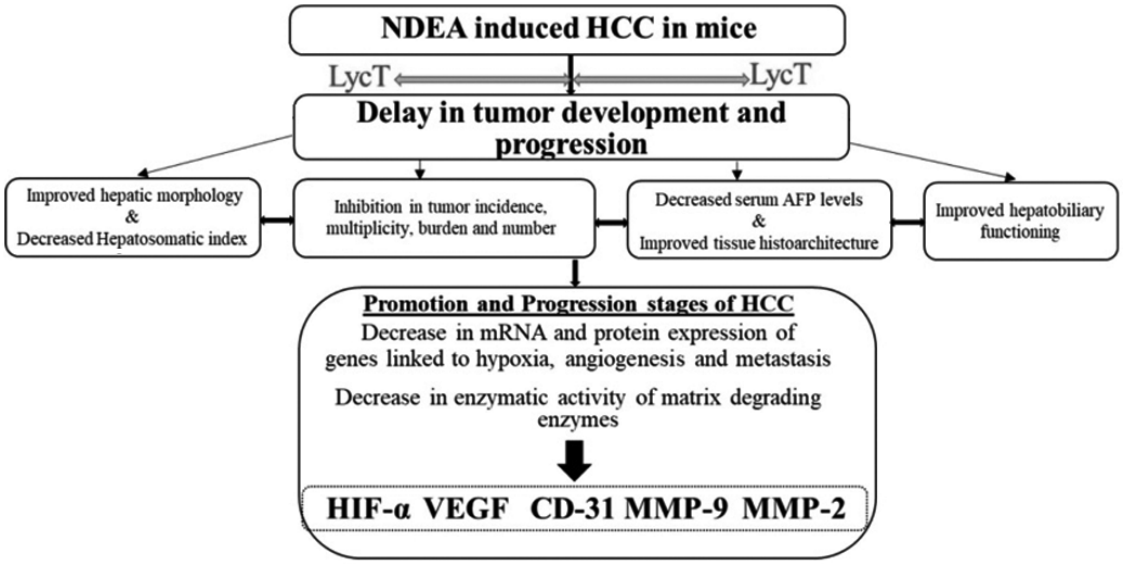

Fig. 10 — Modulatory effects exerted by LycT at late stages of HCC

when compared to control and LycT groups. LycT + NDEA group exhibited marked increase in expression of HIF-α when compared to control and LycT groups and decreased when compared to NDEA group. Protein expression of HIF-α did not differ between the animals of LycT and control groups (Fig. 9C).

MMP-9 and MMP- 2

At 16 and 24 weeks, NDEA group exhibited a significant increase in protein expression of MMPs when compared to control and LycT groups. LycT + NDEA group exhibited marked increase in expression of MMPs when compared to control group and decreased when compared to NDEA group. Protein expression of MMPs did not differ between the animals of LycT and control groups (Fig. 9D & E).

Discussion

The persistent increase in HCC incidence, disease associated mortality and morbidity presses the need for continually exploring newer biomarkers and chemopreventive agents that can effectively and safely minimize the disease burden. The positive results obtained in previous studies prompted us to delve further into some other equally important processes that may be affected during LycT mediated chemoprevention of HCC. This study provides evidence that LycT has the potential to modulate hypoxia, angiogenesis and metastasis at promotion and progression stages. Since evaluation of the functional status of hepatic tissue during HCC is of immense benefit in assessing the disease prognosis, therefore functional status of hepatic tissue was also assessed.

Distorted histoarchitecture was found to be more pronounced in NDEA group than in LycT + NDEA group. The tumors formed in NDEA group were characterized as having a higher histological grade which correlated with the high mortality in these mice. Similar observations were reported earlier by us and others wherein NDEA treatment induced the development of HCC in rodents[9-13,15,21]. It has been previously reported that the cells of undifferentiated HCC seem to have far more invasive potential than that of well-differentiated HCC[22]. In contrast, animals of LycT + NDEA group revealed a delay in the development of HCC as evident from the formation of well-differentiated HCC at 24th week and high grade dysplasia at 16th week. Reduced histopathological alterations were also correlated with the reduction in mortality rate, tumor incidence, multiplicity and burden in mice of LycT + NDEA group. In rats, an inhibition in hepatocarcinogenesis was observed upon supplementation of pure lycopene and tomato extract[23]. Earlier reports from our laboratory also indicated the potential of LycT in mitigating carcinogen induced hepatic damage in mice[10]. Lycopene has been reported to reduce growth of human cancer cell lines by modulating the expression of growth factors and apoptosis associated proteins[24, 25].

Owing to its high sensitivity, serum AFP has been used as a valuable tool for the surveillance of liver

cancer[26]. In the present study, the tenacious increase in AFP level of NDEA group can be correlated with the higher hepatosomatic index, adverse histopathological changes and tumor development and progression. AFP has a prognostic correlation with adverse pathological changes, tumor size, and progression of HCC[26]. In invasive HCC, serum AFP has been reported to interact with carcinoma-associated molecules such as epithelial cellular adhesion molecule (EpCAM)[27]. As reported previously, increased serum AFP level upon NDEA administration has been linked with the metastatic progression of HCC[21]. The decreased AFP levels in mice belonging to LycT + NDEA group indicated slowing down of disease and mitigation in liver damage. Decreased AFP levelswere observed in rats during inhibition of NDEA-phenobarbital induced HCC by *Lycopersicon esculentum*[28].

^{99m}Tc-mebrofenin hepatobiliary function test is often used by clinicians and researchers to evaluate the functional status of liver during various pathologies. We have previously used this test to assess the physiological status of the liver tissue during early stages of HCC[15]. ^{99m}Tc-mebrofenin is actively taken up by the hepatocytes from the systemic circulation and then excreted out into the bile. Animals of control and LycT groups, exhibited normal hepatic uptake and excretion of ^{99m}Tc-mebrofenin. In NDEA group, there was a persistent delay in the uptake and excretion of radioactivity. This indicated that NDEA treatment induced profound perturbations in the functioning of hepatic tissue, thus, delaying the biliary excretion of ^{99m}Tc-mebrofenin. These could also be correlated with the deranged levels of liver function markers and distorted histoarchitecture upon NDEA administration[9-12]. The retention of activity in liver of NDEA mice could be attributed to the obstruction in bile flow or improper functioning of efflux transporters involved in excretion process[29]. In carbon tetrachloride liver injury model, it was observed that cytokine mediated inflammation could be responsible for the extended retention of mebrofenin in the hepatic tissue[30]. In contrast, animals of LycT + NDEA group showed a minor delay in the hepatic uptake which indicated that LycT mitigated NDEA induced hepatic functional perturbations. This could also be attributed to an enhancement in the production and secretion of bile acids upon LycT supplementation that facilitated the rapid excretion of ^{99m}Tc-mebrofenin. These results were also supported by reduced histopathological alterations and improvement of liver markers in LycT administered mice[9-12]. Increased biliary clearance of ^{99m}Tc-mebrofenin was observed during *Azadirachta indica* mediated protection against carcinogen induced hepatic damage[31]. Curcumin administration to rats during hepatitis enhanced the clearance of ^{99m}Tc-mebrofenin thereby suggesting improvement in liver function[32].

In association with hypoxia induced transcription factors [hypoxia inducible factor HIF], hypoxia leads to genetic reprogramming, development of angiogenic phenotype, unique metabolic profile, creation of an immunosuppressive microenvironment *etc*[6]. HCC depends majorly on angiogenesis for metastasis while hypoxia induced glycolysis provides abnormal energy supply for intensively proliferating malignant cells in HCC[33].It has been reported that activation of HIF-1α and β-catenin significantly contributes to the aggressiveness and invasive potential of HCC[34]. HIF-1 consists of two subunits mainly, HIF-1α and HIF-1β, out of which HIF-1α has been implicated in the pathogenesis of liver cancer. Overexpression of HIF-1α may also inhibit apoptosis, thus, leading to the hyper-proliferation of neoplastic cells[35,36].

In the present study, aggressive histopathological changes observed in NDEA group were associated with significant up-regulation of mRNA and protein expression of HIF-1α and VEGF. Delayed HCC development in LycT + NDEA group can be correlated with relatively lower expression of HIF and VEGF in this group.Both VEGF and its receptors VEGFRs, are amongst the most prominent regulators of angiogenesis and are being continually explored as targets in anticancer strategies against several cancer sites including HCC[37]. VEGF acts in an autocrine manner affecting the various cell types with important implications in many liver diseases including HCC[38]. Advanced stages of HCC is featured by heterogeneity in TME which includes hematopoietic precursor cells, bone-marrow derived endothelial cells and cancer stem cells[39,40]. Tumor endothelial cells isolated from several solid tumor masses have been evaluated for several endothelial biomarkers like CD-31. A consistent overexpression of CD-31 during poorly differentiated HCC has been observed[41]. In the present study also, enhanced mRNA and protein expression of CD-31 was

observed in late stages of HCC in NDEA group (Fig. 10). In line with our observations, there are other studies that have linked vascularization and intrahepatic metastases with CD-31 expression in advanced stages of HCC[42]. LycT reduced the angiogenic effect of NDEA as evidenced by decreased CD-31 and VEGF expression in LycT + NDEA group. Systemic review and meta-analysis on various animal models suggested that lycopene regulates the activity of several crucial factors including CD-31, VEGF, HIF *etc*. during initiation and progression of HCC[43,44].

During tumor invasion, degradation and remodelling of stromal architecture by matrix metalloproteinase (MMPs) plays a significant role. MMP-9 and MMP-2 executing type IV collagenase activity have been recognised as main players in degrading the basement membrane during cancer metastasis and invasion[45,46]. Consequently, suppression of such marker proteins can be promising for preventing tumor invasion. MMP-2/9 are substrate-specific gelatinases, and their elevation in serum and hepatic tissues of NDEA group clearly indicated elevated epithelial mesenchymal transition processes corresponding to advanced stages of HCC. Decreased gelatinolytic activity of MMPs in serum and significant lower expression of MMPs in hepatic tissues of LycT + NDEA group, suggested that LycT possibly suppressed metastasis.

The observations of the present study at late stages of HCC and those of the early stages convincingly demonstrate that LycT effectively mitigated hepatic cancer possibly by modulating hypoxia, angiogenesis and metastasis. Such detailed and exhaustive studies done at all stages of tumorigenesis are paramount in establishing the effectiveness of a putative medicinal agent.

Acknowledgement

This work was supported by Department of Science and Technology [Innovation in Science Pursuit for Inspired Research (INSPIRE) IF110576].

Conflict of interest

All authors declare no conflicts of interest.

References

1 Muz B, de la Puente P, Azab F & Azab AK, The role of hypoxia in cancer progression, angiogenesis, metastasis, and resistance to therapy. *Hypoxia (Auckl)*, 3 (2015) 83.

2 Thomlinson RH & Gray LH, The histological structure of some human lung cancers and the possible implications for radiotherapy. *Br J Cancer*, 9 (1955) 539.

3 Semenza GL, Hypoxia. Cross talk between oxygen sensing and the cell cycle machinery. *Am J Physiol Cell Physiol,* 301 (2011) C550.

4 Siegel RL, Miller KD, Fuchs HE & Jemal A, Cancer statistics 2022. *CA Cancer J Clin*, 72 (2022) 7.

5 Philips CA, Rajesh S, Nair DC, Ahamed R, Abduljaleel JK & Augustine P, Hepatocellular Carcinoma in 2021: An Exhaustive Update. *Cureus,* 13 (2021) e19274.

6 Sebestyén A, Kopper L, Dankó T & Tímár J, Hypoxia Signaling in Cancer: From Basics to Clinical Practice. *Pathol Oncol Res,* 27 (2021) 1609802.

7 Rumgay H, Ferlay J, de Martel C, Georges D, Ibrahim AS, Zheng R, Wei W, Lemmens P & Soerjomataram I, Global, regional and national burden of primary liver cancer by subtype. *Eur J Cancer,* 161 (2022) 108.

8 Lange NF, Radu P & Dufour JF, Prevention of NAFLD-associated HCC: Role of lifestyle and chemoprevention. *J Hepatol,* 75 (2021) 1217.

9 Gupta P, Bansal MP & Koul A, Spectroscopic characterization of lycopene extract from *Lycopersicum esculentum* (tomato) and its evaluation as a chemopreventive agent against experimental hepatocarcinogenesis in mice. *Phytother Res,* 27 (2013) 448.

10 Gupta P, Bansal MP & Koul A, Evaluating the effect of lycopene from *Lycopersicum esculentum* on apoptosis during N-nitrosodiethylamine induced hepatocarcinogenesis. *Biochem Biophys Res Commun,* 434 (2013) 479.

11 Gupta P, Bansal MP & Koul A, Lycopene modulates initiation of N Nitrosodiethylamine induced hepatocarcinogenesis: Studies on chromosomal abnormalities, membrane fluidity and antioxidant defense system. *Chemico Biol Interact,* 206 (2013) 364.

12 Gupta P, Bansal MP & Koul A, Lycopene modulates cellular proliferation, glycolysis and hepatic ultra-structure during hepatocellular carcinoma. *World J Hepatol,* 8 (2016) 1222.

13 Bhatia N, Gupta P, Singh B & Koul A, Lycopene enriched tomato extract inhibits hypoxia, angiogenesis, and metastatic markers in early stage N-nitrosodiethylamine induced hepatocellular carcinoma. *Nutr Cancer*, 67 (2015) 1268.

14 Koul A, Shubhrant & Gupta P, Phytomodulatory potential of lycopene from *Lycopersicum esculentum* against doxorubicin induced nephrotoxicity. *Indian J Exp Biol*, 51 (2013)635.

15 Bhatia N, Singh B & Koul A, Lycopene treatment stalls the onset of experimentally induced hepatocellular carcinoma: A radio-isotopic, physiological and biochemical analysis. *Hepatoma Res*, 4 (2018) 9.

16 Humanson GL, In *Basic procedures- Animal tissue technique. Part-I* (Freeman WH, Company CA) 1961, 130.

17 Dignam JD, Lebovitz RM & Roeder RG, Accurate transcription initiation by RNA polymerase II in a soluble extract from isolated mammalian nuclei. *Nucleic Acids Res*, 11 (1983) 1475.

18 Oteiza PI, Clegg MS & Keen CL, Short term zinc deficiency affects NF-κB nuclear binding activity in rat testes. *J Nutr*, 131 (2001) 21

19 Lowry OH, Rosebrough NJ, Farr AN & Randall RJ, Protein measurement with Folin phenol reagent. *J Biol Chem,* 193 (1951) 265.

20 Ito A, Nakajima S, Sasaguri Y, Nagase H & Mori Y, Co-culture of human breast adenocarcinoma MCF-7 cells and human dermal fibroblasts enhance the production of matrix metalloproteinases 1, 2 and 3 in fibroblasts. *Br J Cancer,* 1 (1995) 1039.

21 Keleş OF, Huyut Z, Arslan M, Yıldızhan K & Yener Z, Antitumor activity of *Urtica dioica* seed extract on diethylnitrosamine-induced liver carcinogenesis in rats. *Indian J Biochem Biophys*, 61 (2024) 16.

22 Kojiro M & Roskams T, Early hepatocellular carcinoma and dysplastic nodules. *Sem Liver Dis,* 25 (2005) 133.

23 Wang Y, Ausman LM, Greenberg AS, Russell RM & Wang XD, Dietary lycopene and tomato extract supplementations inhibit nonalcoholic steatohepatitis-promoted hepatocarcinogenesis in rats. *Int J Cancer,* 126 (2010) 1788.

24 Karas M, Amir H, Fishman D, Danilenko M, Segal S, Nahum A, Koifmann A, Giat Y, Levy J & Sharoni Y, Lycopene interferes with cell cycle progression and insulin-like growth factor I signaling in mammary cancer cells. *Nutr Cancer,* 36 (2000) 101.

25 Sathelly K, Kalagatur NK, Mangamuri, Puli COR & Poda S, Anticancer potential of *Solanum lycopersicum* L. extract in human lung epithelial cancer cells A549. *Indian J Biochem Biophys*, 60 (2023) 76.

26 Zhang J, Chen G, Zhang P, ZhangJ, Li X, Gan D, Cao X, Han M, Du H &Ye Y, The threshold of alpha-fetoprotein (AFP) for the diagnosis of hepatocellular carcinoma: A systematic review and meta-analysis. *PLoS One,* 15 (2020) e0228857.

27 Yamashita T, Forgues M, Wang W, Kim JW, Ye Q, Jia H, Budhu A, Zanetti KA, Chen Y, Qin LX, Tang ZY & Wang XW, EpCAM and alpha-fetoprotein expression defines novel prognostic subtypes of hepatocellular carcinoma. *Cancer Res,* 68 (2008) 1451.

28 Das BK, Koti BC & Gadad PC, Role of *Lycopersicon esculentum* in diethylnitrosamine-induced and phenobarbital-promoted hepatocellular carcinoma. *Indian J Health Sci Biomed Res,* 9 (2016) 147.

29 Neyt S, Huisman MT, Vanhove C, De Man H, Vliegen M, Moerman L, Dumolyn C, Mannens G & De Vos F, *In vivo* visualization and quantification of (disturbed) Oatp-mediated hepatic uptake and Mrp2-mediated biliary excretion of ^{99m}Tc-Mebrofenin in mice. *J Nucl Med*, 54 (2013) 624.

30 Joseph B, Bhargava KK, Tronco GG, Kumaran V, Palestro CJ & Gupta S, Regulation of hepatobiliary transport activity and noninvasive identification of cytokine-dependent liver inflammation. *J Nucl Med,* 46 (2005) 146.

31 Koul A, Mohan V & Bharati S, *Azadirachta indica* mitigates DMBA-induced hepatotoxicity: a biochemical and radiometric study. *Indian J Biochem Biophys,* 51 (2014) 37.

32 Deshpande UR, Joseph LJ & Samuel AM, Hepatobiliary clearance of labelled mebrofenin in normal and D-galactosamine HCl-induced hepatitis rats and the protective effect of turmeric extract. *Ind J Physiol Pharmacol,* 47 (2003) 332.

33 Luo D, Wang Z, Wu J, Jiang C & Wu J, The Role of hypoxia inducible factor-1 in hepatocellular carcinoma. *BioMed Res Int,* 2014 (2014) 409272.

34 Shang F, Liu M, Li B, Zhang X, Sheng Y, Liu S, Han J, Li H & Xiu R, The anti-angiogenic effect of dexamethasone in a murine hepatocellular carcinoma model by augmentation of gluconeogenesis pathway in malignant cells. *Cancer Chemother Pharmacol,* 77 (2016) 1087.

35 Liu L, Zhu XD, Wang WQ, Shen Y, Qin Y, Ren ZG, Sun HC & Tang ZY, Activation of beta-catenin by hypoxia in hepatocellular carcinoma contributes to enhanced metastatic potential and poor prognosis. *Clin Cancer Res,* 16 (2010) 2740.

36 Piret JP, Minet E, Cosse JP, Ninane N, Debacq C, Raes M & Michiels C, Hypoxia-inducible factor-1-dependent overexpression of myeloid cell factor-1 protects hypoxic cells against tert-butyl hydroperoxide-induced apoptosis. *J Biol Chem,* 280 (2005) 9336.

37 Niu M, Yi M, Li N, Wu K & Wu K, Advances of Targeted Therapy for Hepatocellular Carcinoma. *Front Oncol,* 11 (2021) 719896.

38 Darmadi D, Ruslie RH & Pakpahan C, Vascular Endothelial Growth Factor (VEGF) in Liver Disease Tumor Angiogenesis and Modulators. IntechOpen, 2022.

39 Bian XW, Wang QL, Xiao HL & Wang JM, Tumor microvascular architecture phenotype (T-MAP) as a new concept for studies of angiogenesis and oncology. *J Neurooncol,* 80 (2006) 211.

40 Ricci-Vitiani L, Pallini R, Biffoni M, Todaro M, Invernici G, Cenci T, Maira G, Parati EA, Stassi G, Larocca LM & De Maria R, Tumour vascularization *via* endothelial differentiation of glioblastoma stem-like cells. *Nature,* 468 (2010) 824.

41 Qian H, Yang L, Zhao W, Chen H & He S, A comparison of CD105 and CD31 expression in tumor vessels of hepatocellular carcinoma by tissue microarray and flow cytometry. *Exper Ther Med,* 16 (2018) 2881.

42 Bösmüller H, Pfefferle V, Bittar Z, Scheble V, Horger M, Sipos B & Fend F, Microvessel density and angiogenesis in primary hepatic malignancies: Differential expression of CD31 and VEGFR-2 in hepatocellular carcinoma and intrahepatic cholangiocarcinoma. *Pathol Res Pract,* 214 (2018) 1136.

43 Mekuria AN, Tura AK, Hagos B, Sisay M, Abdela J, Mishore KM & Motbaynor B, Anti-Cancer Effects of Lycopene in Animal Models of Hepatocellular Carcinoma: A Systematic Review and Meta-Analysis. *Front Pharmacol,* 11 (2020) 1306.

44 Huang H, Hsu S, Chang C, Kao Y, Chuang C, Hou M & Lee F, Lycopene treatment improves intrahepatic fibrosis and attenuates pathological angiogenesis in biliary cirrhotic rats, *J Chin Med Assoc*, 85 (2022) 414.

45 Jiang H & Li H, Prognostic values of tumoral MMP2 and MMP9 overexpression in breast cancer: a systematic review and meta-analysis. *BMC Cancer,* 21 (2021) 149.

46 Niland S, Riscanevo AX & Eble JA, Matrix Metalloproteinases Shape the Tumor Microenvironment in Cancer Progression. *Int J Mol Sci,* 23 (2021) 146.
47 Huang YF, Yang CH, Huang CC & Hsu KS, Vascular endothelial growth factor-dependent spinogenesis underlies antidepressant-like effects of enriched environment. *J Biol Chem,* 287 (2012) 40938.
48 Leng A, Yang J, Liu T, Cui J, Li XH, Zhu Y, Xiong T & Chen Y, Nanoparticle-delivered VEGF-silencing cassette and suicide gene expression cassettes inhibit colon carcinoma growth *in vitro* and *in vivo*. *Tumor Biol,* 32 (2011) 1103.
49 Schmid MC, Bisoffi M, Wetterwald A, Gautschi E, Thalmann GN, Mitola S, Bussolino F & Cecchini MG, Insulin-like growth factor binding protein-3 is overexpressed in endothelial cells of mouse breast tumor vessels. *Int J Cancer,* 103 (2003) 577.
50 Huszarik K, Wright B, Keller C, Nikoopour E, Krougly O, Lee-Chan E, Qin HY, Cameron MJ, Gurr WK, Hill DJ, Sherwin RS, Kelvin DJ & Singh B, Adjuvant immunotherapy increases beta cell regenerative factor Reg2 in the pancreas of diabetic mice. *J Immunol*, 185 (2010) 5120.